Dissipative soliton resonance and noise-like pulse generation of large normal dispersion Yb-doped fiber laser

YUZHAI PAN[1*], HAOXUE QIU[1], TIANQI ZHANG[1], WENJUN LIU[1], JIEGUANG MIAO[1], TIAN ZHAOSHUO[2]

[1]Department of Optoelectronics Science, Harbin Institute of Technology at Weihai,
 Weihai 264209, China

[2]Information Optoelectronics Research Institute, Harbin Institute of Technology at Weihai,
 Weihai 264209, China

*Corresponding author: panyzh2002@163.com

In this paper, we experimentally demonstrate two types of dissipative soliton resonant (DSR) and noise-like pulse (NLP) in a mode-locked fiber laser using the nonlinear optical loop mirror (NOLM). By appropriately adjusting the polarization states, the switchable generation of DSR and NLP can be achieved from one mode-locked fiber laser. By adjusting the pump power, the pulse width of DSR increases gradually from 2.45 to 13.35 ns with a constant peak intensity, while the NLP just has a little increase, even splitting into two narrower pulses at higher pump power. Two types of DSR and NLP have the same pulse periods of 1.29 μs, corresponding to the cavity length of the fiber laser. The obtained results display the evolution process of DSR pulse and NLP in mode-locked fiber laser and have some application in optical sensing, spectral reflectometry, micro-machining, and other relative domains.

Keywords: mode-locked fiber laser, Yb-doped, NOLM, DSR, NLP.

1. Introduction

Passively mode-locked (PML) fiber lasers have attracted much attention in recent years, because of high excellent beam quality, exceptional stability, compact structure, and cost-efficiency [1]. High energy mode-locked pulses in nanosecond time scales have attracted considerable attention and are well used in laser micromachining, optical sensing, optical coherence tomography, optical metrology, and other fields [2–5]. In the past decade, various techniques have been applied to achieve mode locking, for example, nonlinear polarization rotation (NPR) [6, 7], nonlinear optical loop mirror (NOLM) [8, 9], semiconductor saturable absorber mirror [10, 11], nanomaterial-based saturable absorber [12, 13]. In comparison with the above techniques, NOLM has been

extensively studied for its excellent nonlinear switching characteristics and high response speed. And there are rich phenomena and dynamics relating to PML in fiber lasers, besides some typical solitons, that still deserve revelation or further investigating, such as bunched solitons [14], vector solitons [15], bound-state solitons [16], soliton rains [17], soliton molecules [18], dark soliton [19] and so on.

In the continuous research of complex nonlinear dissipative soliton dynamics, researchers have been looking for the appropriate parameters for the mode-locked fiber laser to achieve a stable state mode-locking. Dissipative solitons (DSs) are different from the conventional solitons since they are determined with the balance between positive nonlinearity effect and anomalous fiber dispersion. The formation of DS depends upon gain and loss coexisting in the laser cavity [20, 21]. High energy wave-breaking -free rectangular pulses in nanosecond time scales have attracted considerable attention for their pump-scaled pulse energy without pulse splitting. Recently, dissipative solitons resonances (DSRs) have been investigated in the mode-locking fiber lasers [22, 23]. DSR phenomenon features the generation of a wave-breaking-free flat-top pulse while almost keeping the amplitude constant with the increasing pump power [24]. The reverse saturable absorption played a key role in generating DSR pulses. The pulse width increases fast with a constant height. The chirp range of the pulse becomes larger because the duration of the pulse becomes larger as pump power increases. WANG and coauthors have experimentally demonstrated the generation of DS and DSR pulse with very strong normal cavity dispersion which exists in a passively mode-locked fiber laser [25]. In a large dispersion cavity fiber laser, it tends easily to generate DSR pulse, not DS, due to large group velocity delay and reverse saturable absorption of NOLM.

The polarization state in the fiber cavity can be simply adjusted by the polarization controller (PC) to optimize the stable operation condition. By the changes in the polarization filter effect and the lightwave phase shift different states of the mode-locked pulses as mentioned above can be generated, where the PC is the switcher. Noise-like pulse (NLP) is often generated by the mode-locked fiber laser regardless of the cavity dispersion regime [24, 26–28]. The formation of NLP is more complicated due to fiber birefringence, the soliton instability, and so on. Simultaneous generation of two types of DSR pulses and NLPs in Yb-doped fiber laser takes place with two composite eight -like cavities modulated by two different lengths of NOLM [29]. These different pulses utilize the same gain fiber and pump source. It is useful for simultaneous observation of different dynamics of mode-locked pulses. The NLP has some typical characteristics, like a trail of quasi-stable wave packets of ultrashort sub-pulses and a broader output spectrum, *etc*. How, in the process of increasing the single pulse energy, pulses breaking could occur owing to the excessive nonlinear phase accumulation in a fiber cavity.

In this paper, we have investigated the mode-locking operation of fiber laser in a large normal dispersion regime based on the NOLM. We obtained two types mode-locked pulses of DSR pulse and NLP. By adjusting the polarization states in one fiber lasers cavity via PC, we observed the transition from DSR pulse to NLP and the reverse process. The performances of two types of pulses with the increase of pump power have been demonstrated.

2. The experimental setup

Figure 1 shows the setup of the passively mode-locked fiber laser used in our experiments. The fiber ring cavity is mainly composed of double-cladding Yb-doped fiber (YDF), single-mode fiber, the output coupler, PC and polarization-independent isolator (PI-ISO). Among them, the Yb-doped fiber (Nufern YDF-5/130) has the absorption coefficient of ~0.6 dB/m at the central wavelength of 915 nm and the group velocity dispersion of ~22.1 ps^2/km and a nonlinear coefficient of 0.0048 W^{-1}m^{-1}. The length of the gain fiber is 10 m, which provides a total absorption of around 6 dB, and the end of the YDF was spliced with a single-clad traditional fiber to attenuate the residual pump. The pumping source is a multimode fiber-coupled semiconductor laser with a central output wavelength of 915 nm which is coupled into Yb-doped fiber via the combiner with a coupling efficiency measured to be ~80%. The optical intensity in the laser cavity is periodically modulated by the nonlinear phase shift effect to achieve a stable mode-locking pulse. So, we used 250 m single-mode optical fiber (C1060) to insert into the NOLM composed of a 3 dB beam splitter, which is connected to the ring cavity. The coupler ratio of the 3 dB beam splitter was measured experimentally to be 48.7:51.3. The small ratio difference of the two beams propagating along the opposite direction in the fiber loop would have enough phase difference at higher signal power for the NOLM mode-locking. Another PC here is used to adjust the nonlinear phaseshift effect. The GVD and nonlinear coefficients of the C1060 fiber are ~21.9 ps^2/km and ~0.0075 W^{-1}m^{-1}, respectively. The laser pulse exports through 20% of the 2×1 coupler with a 20:80 ratio. All pigtails were kept the original length as long as ~1 meter, so the total length of the laser ring cavity is about 265 m, and the total dispersion of the cavity is approximately +5.8 ps^2, which is an ultra-large all-positive dispersion cavity.

To synchronously observe the laser pulses characteristics, the output optical signals are divided into two beams by a 2×1 coupler with a beam splitting ratio of 50:50, and the waveform, pulse energy, spectrum of the laser pulses are tested by different testing devices. The laser output was attenuated and measured by a high-speed photoelectric detector (bandwidth is 3 GHz, the rise time is 130 ps) and digital oscilloscope (LeCroy,
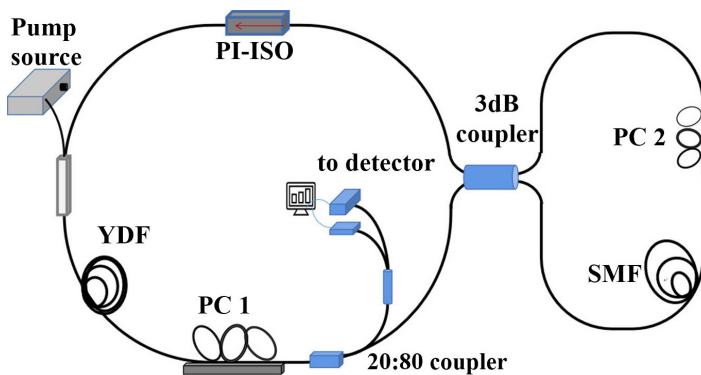

Fig. 1. Structure of the proposed mode-locked fiber laser based on NOLM.

7300A, bandwidth is 3 GHz, the sampling rate is 20 GS/s) with the 3 dB coupler connected. We used the spectrometer (Ocean Optics HR4000) to measure pulse spectrum, used RF spectrum analyzer (GWINSTEK GSP-9330) to analyze the RF characteristics of the pulses, and used optical fiber power meter (JW3216) to measure average output power.

3. Experiment results of different pulsed regimes

3.1. DSR mode-locking pulses

When the pump power is greater than 1.6 W, which is about the threshold power, a stable square-wave DSR pulse could be achieved with the appropriate orientation of the PCs. Stable DSR pulses at the pump power of 1.6 W are shown as in Fig. 2. The profile of a single DSR pulse was measured and presented in Fig. 2**a**. The pulse has a typical rectangular shape with a width of 2.54 ns. As shown in Fig. 2**b**, the corresponding output spectrum has a single peak with a central wavelength of 1077.5 nm and a 3 dB spectral
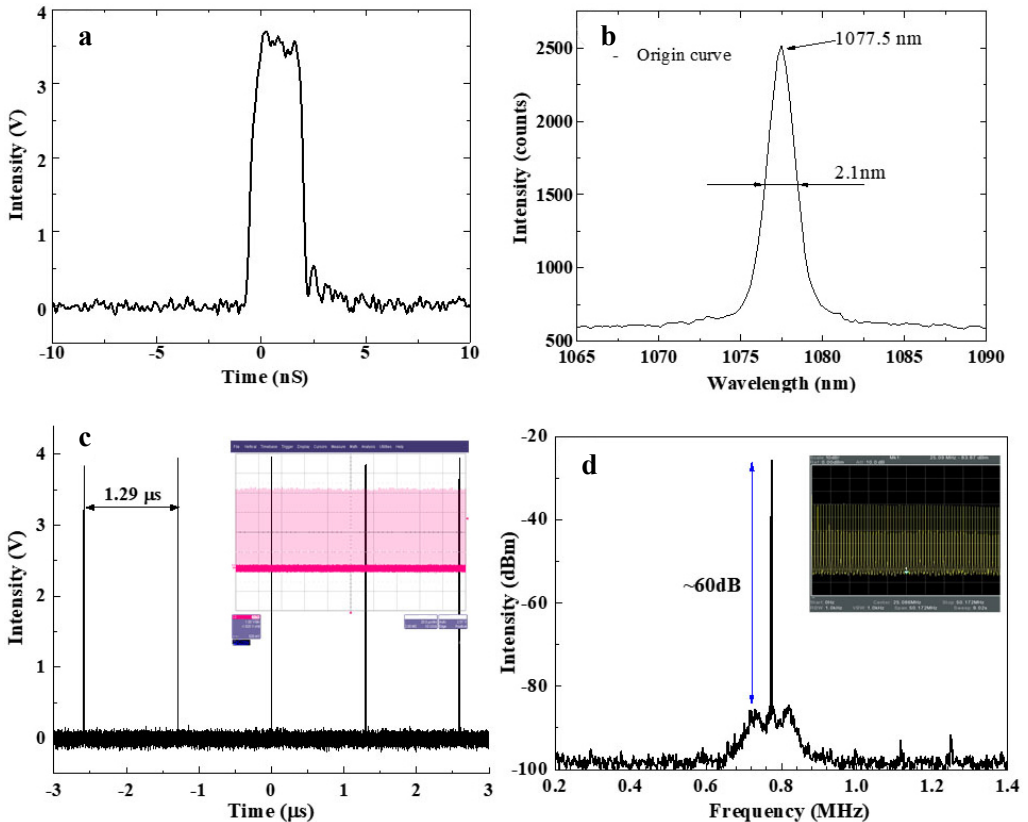

Fig. 2. Output performances of DSR pulses from Yb-doped mode-locked fiber laser. (**a**) Single pulse waveform; (**b**) spectrum; (**c**) pulse sequence diagram, inset: wider pulse trains; and (**d**) radio frequency spectrum, inset: the scanning range of 50 MHz.

bandwidth of 2.1 nm. The pulse spectra show the typical near triangular shape spectrum of DSR pulses. The spectrum indicates the giant chirp of the nanosecond pulses. Figure 2**c** presents the corresponding pulse train with the pulse repetition period is 1.29 μs, which is determined by the cavity length of 265 m. The radio frequency spectrum is showed in Fig. 2**d**, it can be seen that the central frequency is ~774.4 kHz, which is corresponding to the output pulse period in the cavity loop. It is further showed that the laser operates at the fundamental repetition. The signal-to-noise ratio is up to ~60 dB, which displays good stability of the laser pulse train.

We fixed the PC and increased the pump power gradually to further observe the operating state of the mode-locked fiber laser. The mode-locked pulse evolution with the increase of pump power is shown in Fig. 3**a**. The pulse is a rectangular flat-top pulse
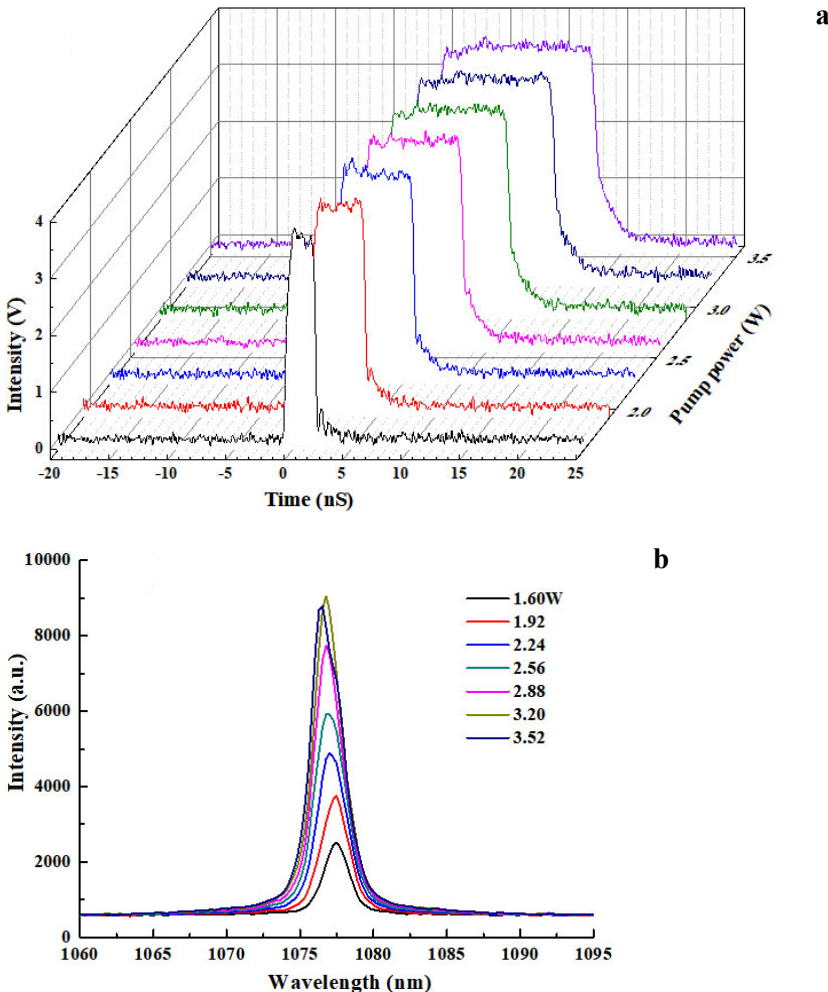

Fig. 3. Time domain waveform (**a**) and the corresponding spectrum (**b**) evolution diagram of the DSR mode-locked pulse with different pump powers.

continually broadens in pulse width, but weakly changes in amplitude. Several pulses were shown in the figure as the increase of pump power from 1.6 to 3.52 W and the pulse width increases gradually from 2.54 to 13.64 ns. It can be observed in Fig. 3**b** that all the spectra are smooth and the spectral intensity increases obviously as the pump power increases.

It can be seen that the duration of the square-wave pulses broadens in a large range of variation with no splitting of the pulse as the increase of pump power, while the peak power of the pulses almost keeps constant. We measured the pulse and got a flat temporal intensity trace by using the GRENOUILLE system (Swamp Optics). When the power changes, the pulse does not split. On the other hand, the corresponding spectra remain single peak structure with a slight blueshift of the central wavelength with the increase of pump power, except for the small jitter of the spectra at 3.52 W. The spectral 3 dB bandwidth around 2.1 nm is increased slightly, which is due to more nonlinear phase accumulations by the self-phase modulation effect. We tried to bend the single -mode fiber slightly, then the pulse and spectrum have a weak shaking at the same time, but the rectangular pulse did not split, and the mode-locked state of the rectangular pulse is maintained unchanged. It is further confirmed that this rectangular pulse is under the operation regime of DSR. This is different from the DS, which is generally manifested as a narrower Gaussian-shaped profile and a wider M-shaped spectrum with the spectral bandwidth up to several ten nanometers. In the DSR regime, most energy stores near the central wavelength, which is forcing the spectrum into a narrower bandwidth, while the DSR pulse normally has a rectangular shape in the time domain due to the lower clamped peak power from more than 250 m cavity of the NOLM [25].

The performance characteristics of the DSR pulse with the increased launched pump power are shown in Fig. 4. It can be seen that the pulse width and the average output power are increased continuously with the increase of pump power. The width of the pulse broadens from 2.45 to 13.35 ns with pump power increasing from 1.60 to 3.52 W. Correspondingly, pulse energy can be expanded from 3.19 to 16.12 nJ. Thinking of the output ratio of 80:20, there are more than 64 nJ of single pulse energy in the fiber cavity.
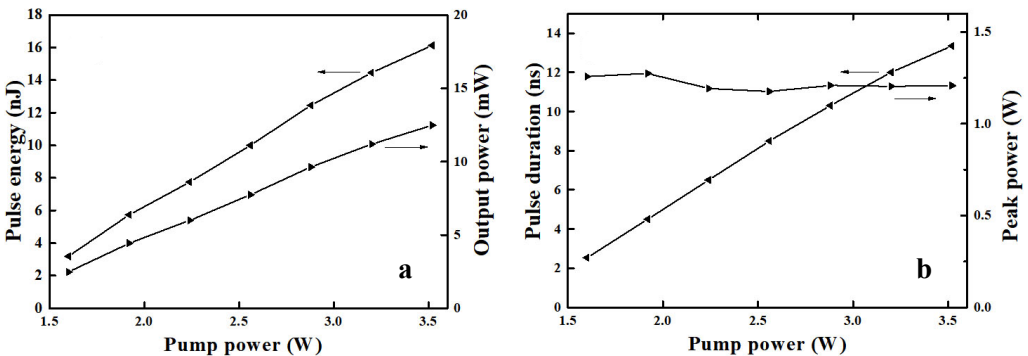

Fig. 4. Measured DSR pulse average output power ad pulse relation between pulse characteristics and pump power.

Here, we did not observe the Raman scattering in the output spectrum in Fig. 3**b**. The corresponding peak power of the pulse is estimated to be ~1.2 W, while the peak power of the pulse nearly remains a constant value. It is because that appropriate laser design allows utilizing the peak power clamping effect induced by the reverse saturable absorption of the NOLM for linear pulse duration tuning via increasing the pump power.

3.2. Noise-like pulse mode locking

Due to the use of the PCs in the NOLM-based mode-locked fiber laser, the polarization state of the propagating light could be changed with the rotation of the PC, and the fiber cavity could act as a Lyot filter by combining the PC and the weak birefringence of the fiber. The different output state can be switched by the PC, which is actually attributed to the nonlinear phase-shift effect.

During the stable mode-locking of the DSR pulse at the pump power of 1.6 W, we changed the orientation of the PC, but we did not find another kind of stable pulses. When the pump power was increased to 1.90 W with an appropriate orientation of the PCs, another stable pulse was realized as depicted in Fig. 5. The pulse profile shown in Fig. 5**a** is different from the DSR pulse, the forefront edge of the pulse is in the same
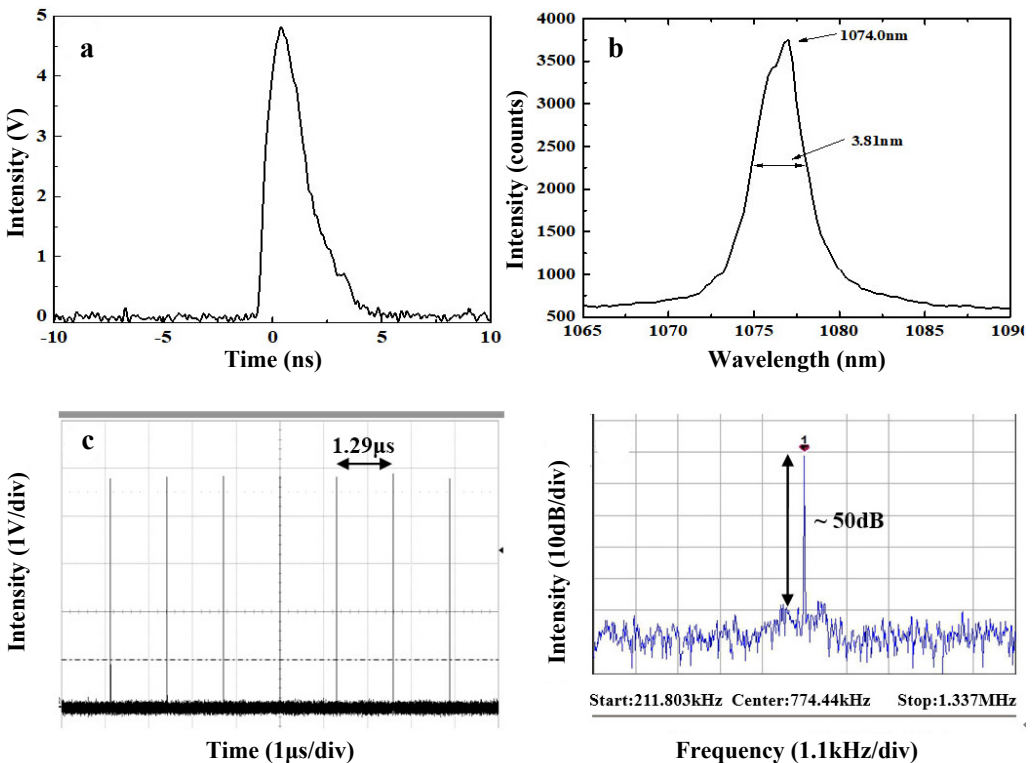

Fig. 5. Experimental observation of NLP laser operation with the pump power of 1.9 W. (**a**) Single pulse, (**b**) spectrum, (**c**) pulse train, and (**d**) radio-frequency spectrum.

sharp-rise state, but the back edge of the pulse decreases slowly, and the pulse shows a narrower width of 1.94 ns. Figure 5**b** shows that the spectrum has the slow descent edges with a central wavelength of 1074.0 nm. The 3 dB bandwidth is 3.81 nm. Both the waveform profile and the spectrum of the pulse show that it operates in the NLP mode -locking regime. Figure 5**c** shows pulse trains measured by an oscilloscope. The interval of adjacent pulses is still 1.29 μs, in accordance with the cavity round-trip time. We also measured the radio-frequency spectrum distribution with a resolution bandwidth of 1 kHz as depicted in Fig. 5**d**. It can be seen that the basic repetition frequency is still approximately 774.4 kHz remarkably and the SNR is about 50 dB, which means that this is another stable mode-locking state from the NOLM-based fiber laser.

To further confirm that the pulse is operated in the NLP regime, the envelope evolution of a single pulse was measured with the increase of pump power and the fixed PCs. The temporal and spectral evolution is presented in Fig. 6. As shown in Fig. 6**a**, when the pump power increased from 1.90 to 2.88 W, the pulse width increased
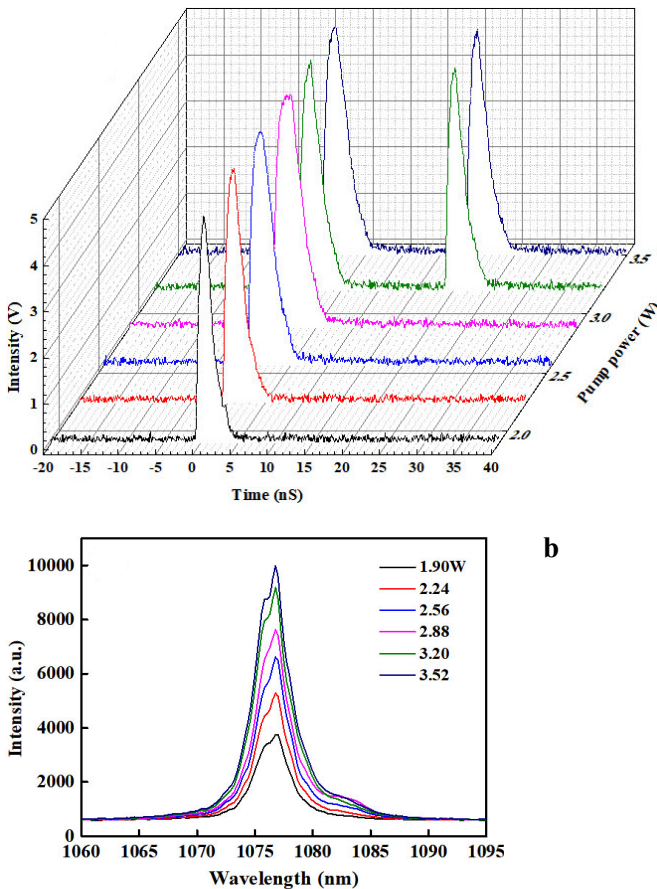

Fig. 6. Time domain waveform (**a**) and the corresponding spectrum (**b**) evolution diagram of NLP with different pump powers.

gradually from 1.94 to 3.76 ns. But from 2.88 to 3.52 W of the pump power, the pulse was split into two sub-pulses with narrower pulse width. When we tried to adjust the PCs slightly at the pump power above 2.88 W, the two sub-pulses could be combined into one unstable near flat-top pulse with a slowly decreasing back edge, which is similar to the characteristics of the rectangular NLP [28, 30], which is not further studied in this paper. During the evolutionary process at different pump power, the shape of the pulses can be kept almost the original spike shape, and the peak intensity of all pulses, which is a little higher than the DSR pulse, remains unchanged. Figure 6**b** gives the corresponding output pulse spectrum with different pump power. The spectrum shows a heterogeneous trapezoidal shape and has the typical characteristics different from the DSR pulse spectrum. With the increase of pump power, the spectrum intensity increases gradually. And the position of the central wavelength of the pulse keeps at about 1076.6 nm. There is no obvious change in the spectrum under single and multi-sub-pulse operation. As the pump power increases, the spectral bandwidth is increased slightly, which is larger than those square-wave DSR pulses. Generally, when the NOLM is adjusted to a low-value power that can modulate the pulse, due to the highly nonlinear effect, the NLP easily tends to split into multiple narrower NLP at the fundamental repetition rate of the laser cavity, that is the repulsive phenomenon against the resonance of dissipative solitons under the different modulation of NOLM [30]. Therefore, we believed that this pulse is operating in the NLP regime.

Comparatively, the switchable performance of mode-locked pulse in a fiber laser cavity is related to the saturable absorption parameters of the NOLM, especially the switching power. The orientation state of the PCs has a significant influence on the parameters of NOLM. Tuning the PC in the experiment, corresponding to increase the switching power, would switch the fiber laser to operate at the NLP regime. Here, higher pump power is required to exceed the switching power to obtain reverse saturable absorption for clamping the peak power.

It seems unreasonable that the pulse width increases with the increase of pump power which is different from the mode-locking principle of the laser. In fact, pulses that can exist at large net cavity GVD rely on the dissipative processes and, therefore, can be considered as dissipative solitons (DSs). The gain and loss coexist in the dissipative system and play an essential role in the formation of DSs. Typically, the time-bandwidth product of the DS is larger than the theoretical value due to the large normal dispersion around 1 μm in the fiber cavity. It has been demonstrated that both the DSR pulse and NLP, appear as a single pulse on the oscilloscope. It has also been shown that they consist of a large number of ultra-short sub-pulses with certain clamped peak powers [24], which arise from the localized background noises or dispersive waves around the outermost pulses from an intrinsic NOLM-mode-locking mechanism when the reverse saturable absorption is enhanced. The ultrashort sub-pulses could split weaker sub-pulses when their peak powers grow beyond their maximums, after accumulating sufficient nonlinear effect in the cavity, which leads the pulses width to broaden as the growth of the pump power. Obviously, the wave packet would appear as a rectangular shape when these ultrashort sub-pulses share the same clamped peak power, which

named the DSR pulse. While in the NLP regime, the accumulated nonlinear effect makes the switching power higher, the newly generated sub-pulses are easily tended to be shaped into pulses with lower peak powers. The weak sub-pulses may display in the back edge of the pulse. The sub-pulses have a weaken cohesion and form quasi-stable state with a fluctuating internal structure.

DSR pulse is known as a competitive high energy pulse for obtaining high peak power via linear chirp compression due to little higher-order group velocity dispersion of DSR pulse. But the NLP has the higher peak power pulse energy, and a broader spectrum, so the NLP can be applied in low-coherence spectral reflectometry, micromachining, and efficient supercontinuum generation as mentioned above.

4. Conclusion

In conclusion, we have reported on the generation of DSR and NLP in NOLM mode -locked Yb-doped fiber laser. The cavity configuration of the proposed fiber laser produced two distinctive types of pulses at the same cavity. Two types of pulses operation at different pump power have been observed experimentally. DSR pulse has a central wavelength of 1077.5 nm with a 3 dB bandwidth of 2.1 nm, while the NLP has a central wavelength of 1074 nm with a 3 dB bandwidth of 3.81 nm. Both types of pulse have the same pulse periods of 1.29 μs, that is the fundamental repetition frequency of 774.4 kHz, due to one fiber laser cavity. The orientation of the PC has great influence on the switching of different mode-locking regimes. The obtained results improve the understandind of the evolutionary process of DSR pulses and NLPs in the mode-locked fiber laser with NOLM.

Disclosures
The authors declare no conflicts of interest.

References

[1] Fermann M.E., Hartl I., *Ultrafast fiber lasers*, Nature Photonics **7**, 2013, pp. 868–874, DOI: 10.1038/nphoton.2013.280.

[2] Özgören K., Öktem B., Yilmaz S., Ilday F.Ö., Eken K., *83 W, 3.1 MHz, square-shaped, 1 ns-pulsed all-fiber-integrated laser for micromachining*, Optics Express **19**(18), 2011, pp. 17647–17652, DOI: 10.1364/OE.19.017647.

[3] Cranch G.A., Flockhart G.M.H., Kirkendall C.K., *Efficient fiber Bragg grating and fiber Fabry –Perot sensor multiplexing scheme using a broadband pulsed mode-locked laser*, Journal of Lightwave Technology **23**(11), 2005, pp. 3798–3807, DOI: 10.1109/JLT.2005.857735.

[4] Yu X., Luo J., Xiao X.S., Wang P., *Research progress of high-power ultrafast fiber lasers*, Chinese Journal of Lasers **46**(5), 2019, article 0508007 (in Chinese).

[5] HERNANDEZ-GARCIA J.C., ESTUDILLO-AYALA J.M., POTTIEZ O., FILOTEO-RAZO J.D., LAUTERIO-CRUZ J.P., SIERRA-HERNANDEZ J.M., ROJAS-LAGUNA R., *Flat supercontinuum generation by a F8L in high-energy harmonic noise-like pulsing regime*, Laser Physics Letters **13**(12), 2016, article 125104, DOI: 10.1088/1612-2011/13/12/125104.

[6] DONG Z.K., SONG Y.R., XU R.Q., ZHENG Y., TIAN J., LI K., *Broadband spectrum generation with compact Yb-doped fiber laser by intra-cavity cascaded Raman scattering*, Chinese Optics Letters **15**(7), 2017, article 071408.

[7] PAN W.W., ZHANG L., ZHOU J.Q., YANG X., FENG Y., *Raman dissipative soliton fiber laser pumped by an ASE source*, Optics Letters **42**(24), 2017, pp. 5162–5165, DOI: 10.1364/OL.42.005162.

[8] CHESTNUT D.A., TAYLOR J.R., *Wavelength-versatile subpicosecond pulsed lasers using Raman gain in figure-of-eight fiber geometries*, Optics Letters **30**(22), 2005, pp. 2982–2984, DOI: 10.1364/OL.30.002982.

[9] AGUERGARAY C., MÉCHIN D., KRUGLOV V., HARVEY J.D., *Experimental realization of a mode-locked parabolic Raman fiber oscillator*, Optics Express **18**(8), 2010, pp. 8680–8687, DOI: 10.1364/OE.18.008680.

[10] CHAMOROVSKIY A., RAUTIAINEN J., LYYTIKÄINEN J., RANTA S., TAVAST M., SIRBU A., KAPON E., OKHOTNIKOV O.G., *Raman fiber laser pumped by a semiconductor disk laser and mode locked by a semiconductor saturable absorber mirror*, Optics Letters **35**(20), 2010, pp. 3529–3531, DOI: 10.1364/OL.35.003529.

[11] GUO B., XIAO Q., WANG S., ZHANG H., *2D layered materials: synthesis, nonlinear optical properties, and device applications*, Laser & Photonics Reviews **13**(12), 2019, article 1800327, DOI: 10.1002/lpor.201800327.

[12] ZHU P., SANG M., WANG X.L., *et al.*, *A passive mode-locking pulse fiber laser based on single-walled carbon nanotube saturable absorber*, Journal of Optoelectronics Laser **23**(9), 2012, pp. 1686–1690 (in Chinese).

[13] WANG Y.B., QI X.H., SHEN Y., YAO Y.L., XU Z.J., PAN Y.Z., *Ultra-long cavity multi-wavelength Yb-doped fiber laser mode-locked by carbon nanotubes*, Acta Physica Sinica **64**(20), 2015, article 204205, DOI: 10.7498/aps.64.204205.

[14] CHEN Y., WU M., TANG P., CHEN S., DU J., JIANG G., LI Y., ZHAO C., ZHANG H., WEN S., *The formation of various multi-soliton patterns and noise-like pulse in a fiber laser passively mode-locked by a topological insulator based saturable absorber*, Laser Physics Letters **11**(5), 2014, article 055101, DOI: 10.1088/1612-2011/11/5/055101.

[15] SONG Y., CHEN S., ZHANG Q., LI L., ZHAO L., ZHANG H., TANG D., *Vector soliton fiber laser passively mode locked by few layer black phosphorus-based optical saturable absorber*, Optics Express **24**(23), 2016, pp. 25933–25942, DOI: 10.1364/OE.24.025933.

[16] WANG Z., XU Y., DHANABALAN S.C., SOPHIA J., ZHAO C., XU C., XIANG Y., LI J., ZHANG H., *Black phosphorus quantum dots as an efficient saturable absorber for bound soliton operation in an erbium doped fiber laser*, IEEE Photonics Journal **8**(5), 2016, article 1503310, DOI: 10.1109/JPHOT.2016.2598085.

[17] CHOULI S., GRELU P., *Rains of solitons in a fiber laser*, Optics Express **17**(14), 2009, pp. 11776–11781, DOI: 10.1364/OE.17.011776.

[18] LIU X., YAO X., CUI Y., *Real-time observation of the buildup of soliton molecules*, Physical Review Letters **121**(2), 2018, article 023905, DOI: 10.1103/PhysRevLett.121.023905.

[19] ZHANG H., TANG D.Y., ZHAO L.M., WU X., *Dark pulse emission of a fiber laser*, Physical Review A **80**(4), 2009, article 045803, DOI: 10.1103/PhysRevA.80.045803.

[20] ZHAO L.M., TANG D.Y., CHENG T.H., LU C., *Nanosecond square pulse generation in fiber lasers with normal dispersion*, Optics Communications **272**(2), 2007, pp. 431–434, DOI: 10.1016/j.optcom.2006.11.035.

[21] WISE F.W., CHONG A., RENNINGER W.H., *High-energy femtosecond fiber lasers based on pulse propagation at normal dispersion*, Laser & Photonics Reviews **2**(1–2), 2008, pp. 58–73, DOI: 10.1002/lpor.200710041.

[22] CHANG W., ANKIEWICZ A., SOTO-CRESPO J.M., AKHMEDIEV N., *Dissipative soliton resonances*, Physical Review A **78**(2), 2008, article 023830, DOI: 10.1103/PhysRevA.78.023830.

[23] CHENG Z., LI H., WANG P., *Simulation of generation of dissipative soliton, dissipative soliton resonance and noise-like pulse in Yb-doped mode-locked fiber lasers*, Optics Express **23**(5), 2015, pp. 5972 –5981, DOI: 10.1364/OE.23.005972.

[24] DENG Z.S., ZHAO G.K., YUAN J.Q., LIN J.P., CHEN H.J., LIU H.Z., LUO A.P., CUI H., LUO Z.C., XU W.C., *Switchable generation of rectangular noise-like pulse and dissipative soliton resonance in a fiber laser*, Optics Letters **42**(21), 2017, pp. 4517–4520, DOI: 10.1364/OL.42.004517.

[25] LIN W., WANG S.M., XU S., LUO Z.C., YANG Z., *Analytical identification of soliton dynamics in normal-dispersion passively mode-locked fiber lasers: from dissipative soliton to dissipative soliton resonance*, Optics Express **23**(11), 2015, pp. 14860–14875, DOI: 10.1364/OE.23.014860.

[26] TANG D.Y., ZHAO L.M., ZHAO B., *Soliton collapse and bunched noise-like pulse generation in a passively mode-locked fiber ring laser*, Optics Express **13**(7), 2005, pp. 2289–2294, DOI: 10.1364/OPEX. 13.002289.

[27] ZHAO L.M., TANG D.Y., WU J., FU X.Q., WEN S.C., *Noise-like pulse in a gain-guided soliton fiber laser*, Optics Express **15**(5), 2007, pp. 2145–2150, DOI: 10.1364/OE.15.002145.

[28] DONG T., LIN J., ZHOU Y., GU C., YAO P., XU L., *Noise-like square pulses in a linear-cavity NPR mode-locked Yb-doped fiber laser*, Optics & Laser Technology **136**, 2021, article 106740, DOI: 10.1016/j.optlastec.2020.106740.

[29] LIANG F., DONG Z., CUI Y., TIAN J., SONG Y., *Simultaneous generation of two types of pulse shape in an Yb-doped fiber laser system*, IEEE Photonics Technology Letters **32**(), 2020, pp. 259–262, DOI: 10.1109/LPT.2020.2970804.

[30] HUANG Y.Q., QI Y.L., LUO Z.C., LUO A.P., XU W.C., *Versatile patterns of multiple rectangular noise-like pulses in a fiber laser*, Optics Express **24**(7), 2016, pp. 7356–7363, DOI: 10.1364/OE.24.007356.